Scripta Materialia 159 (2018) 94–98

Contents lists available at ScienceDirect

Scripta Materialia

journal homepage: www.elsevier.com/locate/scriptamat

Tracer diffusion in the Ni–CoCrFeMn system: Transition from a dilute solid solution to a high entropy alloy

Josua Kottke[a,*], Mathilde Laurent-Brocq[b], Adnan Fareed[a], Daniel Gaertner[a], Loïc Perrière[b], Łukasz Rogal[c], Sergiy V. Divinski[a,*], Gerhard Wilde[a]

[a] Institute of Materials Physics, University of Münster, Münster D-48149, Germany
[b] Université Paris Est, CNRS, UPEC, ICMPE (UMR 7182), Thiais F-94320, France
[c] Institute of Metallurgy and Materials Science, Polish Academy of Sciences, 30-059 Krakow, Poland

ARTICLE INFO

Article history:
Received 13 July 2018
Received in revised form 31 August 2018
Accepted 8 September 2018
Available online xxxx

Keywords:
High entropy alloy
Diffusion
Bulk diffusion

ABSTRACT

Tracer diffusion of Co, Cr, Fe and Ni is measured at 1373 K in $Co_{20}Cr_{20}Fe_{20}Mn_{20}Ni_{20}$, $Co_{10}Cr_{10}Fe_{10}Mn_{10}Ni_{60}$ and $Co_2Cr_2Fe_2Mn_2Ni_{92}$ alloys. Diffusion retardation in the high-entropy $Co_{20}Cr_{20}Fe_{20}Mn_{20}Ni_{20}$ alloy is most prominent in comparison to the $Co_2Cr_2Fe_2Mn_2Ni_{92}$ solid solution, however the concept of 'sluggish' diffusion cannot be used as a blanket statement. The tracer diffusion coefficient drops either slightly (by a factor of three, Fe) or marginally (by a factor of 1.2, Ni) if compared at 1373 K. Alternatively, if compared on a homologous temperature scale, the diffusion retardation can be as large as a factor of 30 (Fe) or 10 (Ni).

Alloys have traditionally been developed according to a 'base element' paradigm, where one element of the alloy is predominant, e.g. iron in steel and nickel in super alloys, and other elements are taken to improve their properties [1]. In 2004, a new concept was introduced [2,3] and, since then, alloys with multiple principal elements and the concentration of each element between 5 and 35 at.%, still forming a solid solution, have been investigated. These alloys are known as multi-principal-element alloys or further as high-entropy alloys (HEAs) [4]. The last name goes back to Yeh et al. [2]. Some of these HEAs have exhibited very promising mechanical properties [5,6], thus initiating a very dynamic field of research. Step by step, properties of HEAs are explored and one of primary importance is diffusion. Indeed, diffusion is of interest for basic research as well as for applications since it is related with the atomic structure and electronic interactions, but at the same time controls phase formation or degradation of materials.

A concept of 'sluggish' diffusion in HEAs in comparison to conventional alloys was proposed as one of the four 'core effects' of HEAs [7]. The first interdiffusion measurements on the Co–Cr–Fe–Mn–Ni alloys seemed to support this paradigm [8].[1] However, for the past two years, the concept of 'sluggish' diffusion has been questioned [4,12-15]. Moreover, the latest diffusion measurements on HEAs have shown that the determination whether diffusion in HEAs is sluggish or not is not straightforward [14].

In fact, the term 'sluggish' diffusion is vaguely defined, since the reference is ambiguous. So far, the diffusion rates in HEAs were compared to those in pure elements or (nearly) equiatomic alloys. Solid solutions, including concentrated ones, present further systems, which might be relevant. In this case one may differentiate the effects of vacancy–solute binding and those of the variable environments of a vacancy in a high-entropy alloy. Furthermore, the diffusivities have to be compared on both, absolute and homologous temperature scales. For an overview of the recent progress on this topic see e.g. Ref. [9].

In the present study, we focus on the comparison of the diffusion rates of elements in multi-principal element alloys within the same system when the composition is varied from pure metal to a dilute solid solution and finally to a HEA. Thus, the influence of

* Corresponding authors.
E-mail addresses: josua.kottke@uni-muenster.de (J. Kottke), divin@wwu.de (S.V. Divinski).

[1] However, serious drawbacks in the original analysis of the interdiffusion data were found [9], see also the discussion in [10,11].

https://doi.org/10.1016/j.scriptamat.2018.09.011
1359-6462/

the element concentration on diffusion in HEAs can be determined without having to take into account the influence of the nature of the elements. This approach could clarify the 'sluggish diffusion' core effect of HEAs. To this end, three alloys containing the same chemical elements in different proportions, namely $Co_{20}Cr_{20}Fe_{20}Mn_{20}Ni_{20}$, $Co_{10}Cr_{10}Fe_{10}Mn_{10}Ni_{60}$ and $Co_2Cr_2Fe_2Mn_2Ni_{92}$ were selected. Those three alloys were already proven to form single face-centered cubic (FCC) solid solutions [16-18]. The first is the widely studied so-called Cantor HEA. The last one is a conventional dilute solid solution, where Ni is the main element and Co, Cr, Fe and Mn are solutes. The composition of the $Co_{10}Cr_{10}Fe_{10}Mn_{10}Ni_{60}$ alloy is in between an equimolar HEA and a conventional alloy. Its purpose is to identify a possible discontinuity (if it exists) in the evolution of the diffusion properties, which would reflect a specificity of HEAs.

The $Co_{10}Cr_{10}Fe_{10}Mn_{10}Ni_{60}$ and $Co_2Cr_2Fe_2Mn_2Ni_{92}$ alloys were prepared by the same procedure: First, Co, Cr, Fe, Mn and Ni metal pieces of at least 99.95% purity were melted by high frequency electromagnetic induction melting in a water-cooled copper crucible under He atmosphere. Then, suction casting was performed to shape the ingots into a rod with a diameter of 13 mm. Rods were wrapped in Ta foil and annealed at 1373 K for 13 h under a He atmosphere for chemical homogenization. Afterwards, the ingots were cold-rolled with a thickness reduction of 70–80 %, to obtain sheets with a thickness of 0.7 to 1 mm suitable for the diffusion measurements.

A five-component equiatomic HEA was manufactured using elemental ingredients of Co, Cr, Fe, Mn and Ni of 99.9% purity in an inductive furnace (Balzer, VSG-50) under a protective Ar atmosphere. During the process, Co, Fe, Mn and Ni were first melted and then Cr was added to the liquid alloy (due to the possibility of covering Cr pieces with oxides during the slow heating process in the furnace). Taking into consideration the probability of Mn evaporation, its amount was increased by 1%. The samples were cast in a steel mold, pre-heated to 473 K, and rods of 20 mm diameter and 100 mm length were obtained. The samples were homogenized by annealing at 1473 K for 50 h.

Discs of 5–6 mm diameter were cut by spark erosion, wrapped in Ta foil, sealed in quartz ampoules under purified Ar atmosphere and annealed at 1423 K for 3 days allowing recrystallization to occur. One face of each sample was ground and polished first mechanically and finally chemically to a mirror-like finish. All samples were annealed at the intended diffusion annealing temperature (1373 K) for the diffusion annealing time (1 month) to achieve equilibrium defect concentrations.

The microstructure was characterized by scanning electron microscopy (SEM, FEI Nova NanoSEM 230) using energy-dispersive X-ray spectroscopy (EDS) and electron backscatter diffraction (EBSD), as well as by X-ray diffraction (XRD, Siemens D5000). A Netzsch DSC 404 F1 Pegasus calorimeter was used to perform Differential Scanning Calorimetry (DSC). Around 100 mg of each composition was put into an alumina crucible and heated up to 1773 K at a rate of 20 K/min under an Ar flow, afterwards, the crucibles were cooled down to room temperature at the same rate. When the same heating cycle is reproduced several times, the relative difference of the determined solidus and liquidus temperatures is lower than 0.1%.

Few microliters of a mixture of γ-isotopes, ^{51}Cr, ^{57}Co and ^{59}Fe, with the partial activities between 6 and 10 kBq, were dropped on the flat, etched surface of annealed samples. ^{63}Ni tracer solution (a β-isotope) was separately deposited on a second set of samples. The samples were wrapped in Ta foil, sealed into high purity silica tubes, evacuated first to a residual pressure below 10^{-5} mbar and backfilled with Ar, and diffusion annealed for 1 month at 1373 K. Afterwards, the discs were reduced in diameter to exclude the influence of surface and/or lateral diffusion. The penetration profiles were measured by parallel sectioning using precise mechanical grinding. The thickness of each section was determined by the mass difference before and after grinding. The relative specific activity of each section, which is proportional to the tracer concentration, was measured using a Liquid Scintillation Analyzer for the β-tracer (^{63}Ni) and an intrinsic Ge γ-detector for the γ-tracers (^{51}Cr, ^{57}Co and ^{59}Fe). The counting time was chosen to approach 2% statistical accuracy.

After the homogenization annealing, XRD (Fig. 1a) revealed that $Co_{20}Cr_{20}Fe_{20}Mn_{20}Ni_{20}$, $Co_{10}Cr_{10}Fe_{10}Mn_{10}Ni_{60}$ and $Co_2Cr_2Fe_2Mn_2Ni_{92}$ alloys are composed of a single phase FCC solid solution. A SEM-EDS analysis (step size of 100 nm) proved elemental homogeneity in all alloys and has not detected precipitates or element enrichment at grain boundaries after annealing at 1373 K.

The lattice parameters of $Co_{20}Cr_{20}Fe_{20}Mn_{20}Ni_{20}$, $Co_{10}Cr_{10}Fe_{10}Mn_{10}Ni_{60}$ and $Co_2Cr_2Fe_2Mn_2Ni_{92}$ are 3.598 ± 0.001, 3.585 ± 0.003 and 3.543 ± 0.001 Å, respectively. Those results are in agreement with the previous work [16,18]. The samples were also characterized by SEM after cold-rolling and recrystallization annealing. As expected, large recrystallized grains were formed with an average size larger than 300 μm. Due to considerable large grains, a probable contribution of grain boundary diffusion is decreased. The SEM inspection with EBSD revealed a high fraction of high-angle grain boundaries, although numerous twin boundaries were also observed after the annealing treatment.

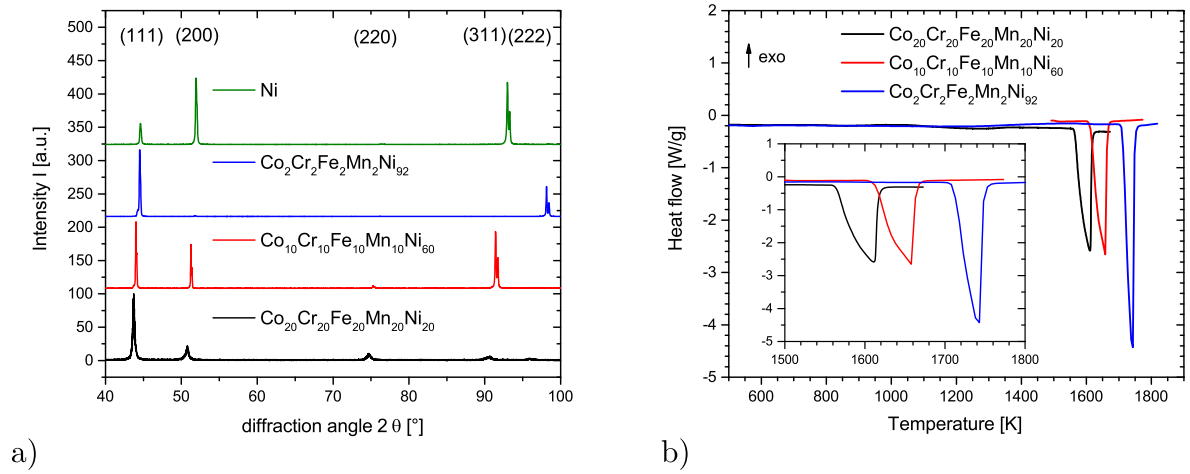

Fig. 1. Normalized X-ray diffraction patterns of $Co_{20}Cr_{20}Fe_{20}Mn_{20}Ni_{20}$, $Co_{10}Cr_{10}Fe_{10}Mn_{10}Ni_{60}$, $Co_2Cr_2Fe_2Mn_2Ni_{92}$ and pure Ni. The crystallographic planes of the FCC phase are indicated above the corresponding peaks. The peak shifts are explained by varying lattice parameters [18]. DSC curves of $Co_{20}Cr_{20}Fe_{20}Mn_{20}Ni_{20}$, $Co_{10}Cr_{10}Fe_{10}Mn_{10}Ni_{60}$ and $Co_2Cr_2Fe_2Mn_2Ni_{92}$ alloys. The inset on the bottom left is a zoom of the endothermic peaks, which represent the melting process.

Table 1
Volume diffusion coefficients for $Co_xCr_xFe_xMn_xNi_{100-4x}$ alloys at 1373 K.

Alloy	T_m K	D_V for ^{51}Cr 10^{-15} m^2/s	D_V for ^{57}Co 10^{-15} m^2/s	D_V for ^{59}Fe 10^{-15} m^2/s	D_V for ^{63}Ni 10^{-15} m^2/s
$Co_{20}Cr_{20}Fe_{20}Mn_{20}Ni_{20}$	1611	$4.0^{+0.7}_{-0.5}$	$1.4^{+0.5}_{-0.1}$	$2.9^{+0.2}_{-0.5}$	$1.6^{+0.6}_{-0.2}$
$Co_{10}Cr_{10}Fe_{10}Mn_{10}Ni_{60}$	1659	$6.1^{+0.5}_{-0.2}$	$3.2^{+0.2}_{-0.1}$	$5.5^{+0.3}_{-0.1}$	$2.4^{+0.3}_{-0.3}$
$Co_2Cr_2Fe_2Mn_2Ni_{92}$	1743	$8.4^{+1.0}_{-1.2}$	$3.5^{+0.3}_{-0.4}$	$7.8^{+1.3}_{-0.8}$	$1.9^{+0.3}_{-0.7}$

In order to be able to compare the diffusion coefficients on a homologous temperature scale, the melting points of the three alloys were measured by DSC. During heating between room temperature and 1773 K, a single endothermic peak, which corresponds to the melting, was recorded for the three alloys (Fig. 1b). As previously proposed [12], the liquidus temperature is chosen to represent the melting point and is determined at the maximum of the peak. The values are given in Table 1 and plotted in Fig. 2b. The melting point decreases from (1743 ± 1) K for $Co_2Cr_2Fe_2Mn_2Ni_{92}$ to (1611 ± 2) K for $Co_{20}Cr_{20}Fe_{20}Mn_{20}Ni_{20}$.

Exemplarily, the penetration profiles of ^{51}Cr, ^{57}Co and ^{59}Fe diffusion in the $Co_{10}Cr_{10}Fe_{10}Mn_{10}Ni_{60}$ alloy are shown in Fig. 2a by plotting the logarithm of the relative specific activity of the tracer, c, against the diffusion length squared, y^2. All penetration profiles are of a similar quality. A linear decrease of the tracer concentration in the given coordinates can be followed to the penetration depths of 300 to 500 μm. Accordingly, the instantaneous source solution of the diffusion problem [19],

$$c(y,t) = \frac{M}{\sqrt{\pi D_V t}} \exp\left(-\frac{y^2}{4D_V t}\right) \quad (1)$$

is fulfilled. Here t is the diffusion annealing time and D_V the volume diffusion coefficient. M denotes the initial amount of tracer material applied to the external surface. Due to the linearity of the profiles in Gaussian coordinates, the volume diffusion coefficients, D_V, can directly be determined:

$$D_V = \frac{1}{4t}\left(-\frac{\partial \ln c(y,t)}{\partial y^2}\right)^{-1}. \quad (2)$$

All investigated elements provided reliable penetration profiles for the diffusion time used, for which the relative uncertainty is between 3 and 32% respectively for Fe and Co. The determined volume diffusion coefficients are given in Table 1 and plotted in Fig. 2b as functions of the Ni concentration (the left ordinate).

For $Co_{10}Cr_{10}Fe_{10}Mn_{10}Ni_{60}$, $Co_2Cr_2Fe_2Mn_2Ni_{92}$ and for pure Ni, the diffusion coefficients at 1373 K can be ranked similarly: $D_V(Cr) \approx D_V(Fe) > D_V(Co) > D_V(Ni)$. Furthermore, in $Co_{20}Cr_{20}Fe_{20}Mn_{20}Ni_{20}$ and $Co_{10}Cr_{10}Fe_{10}Mn_{10}Ni_{60}$, $D_V(Co)$ and $D_V(Ni)$ are found to be similar at 1373 K.

In Fig. 3, the present results on the high-entropy $Co_{20}Cr_{20}Fe_{20}Mn_{20}Ni_{20}$ alloy are compared to the previous measurements, including the data on radiotracer diffusion on a coarse-grained polycrystalline alloy from Vaidya et al. [14], radiotracer diffusion on a single crystalline alloy from Gaertner et al. [24] and the diffusion couple measurements on a polycrystalline alloy by Tsai et al. [8]. Thus, different diffusion measurement techniques and processing routes are compared. The relative standard deviations between those four studies range from 13% to 25% respectively for Ni and Co. These deviations correspond roughly to the measurement uncertainties. Still,

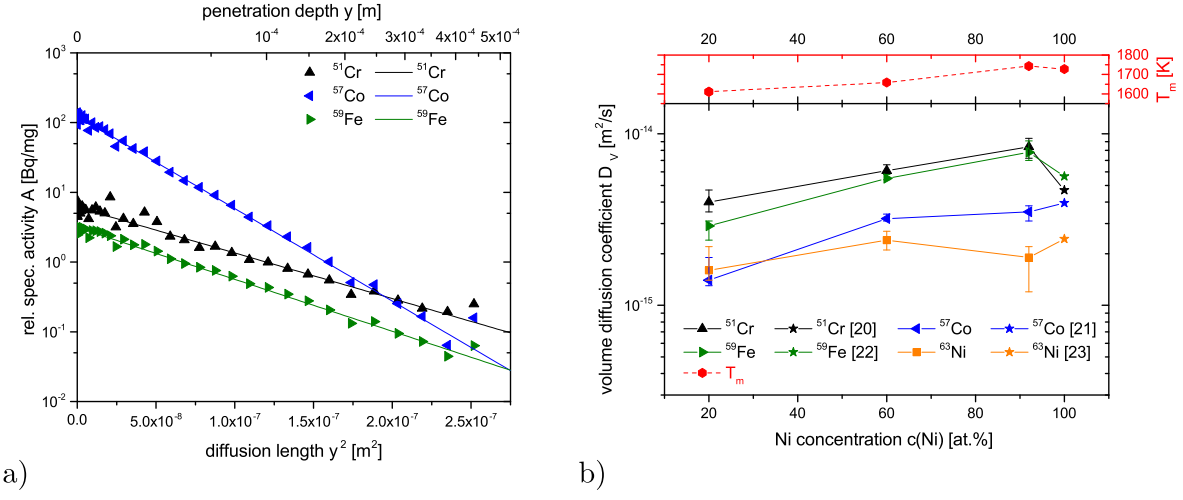

Fig. 2. (a) Examples of penetration profiles measured for ^{51}Cr, ^{57}Co and ^{59}Fe diffusion in the $Co_{10}Cr_{10}Fe_{10}Mn_{10}Ni_{60}$ alloy. The Gaussian fits are plotted by solid lines. The penetration profiles of all investigated alloys are of a similar quality for all isotopes. (b) Volume diffusion coefficients of the constituent elements at 1373 K as functions of Ni content in the three studied alloys (left ordinate). For comparison, the melting point of the alloys are plotted as red pentagons (red ordinate on the right side). Data for pure Ni are plotted for comparison [20-23].

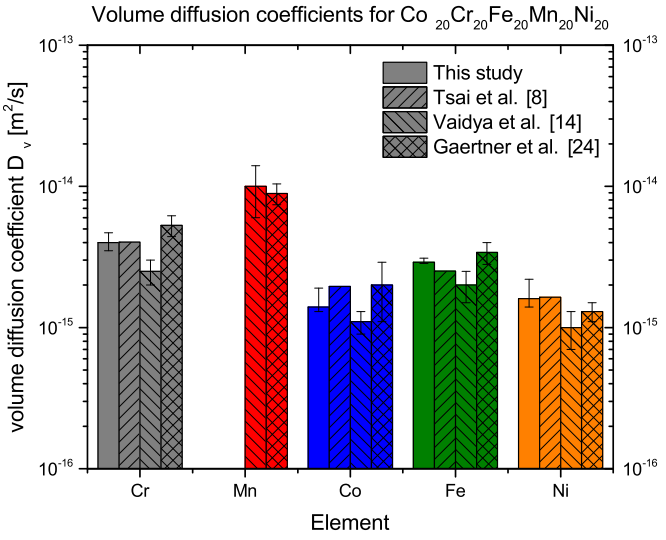

Fig. 3. Comparison of volume diffusion D_V measured at 1373 K in the $Co_{20}Cr_{20}Fe_{20}Mn_{20}Ni_{20}$ alloy. D_V were measured by radiotracer diffusion on polycrystalline alloys (this study, Vaidya et al. [14]), by radiotracer diffusion on a single crystalline alloy (Gaertner et al. [24]) and by a diffusion couple consisting of polycrystalline alloys (Tsai et al. [8]). The error bars correspond to deviations between maximal and minimal Gaussian solutions of the profiles (see Eq. (2)). D_V(Mn) was not measured in this study.

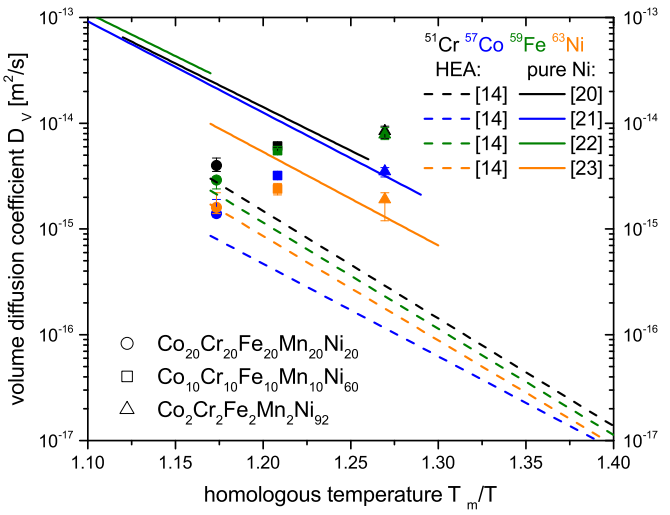

Fig. 4. Volume diffusion of Cr, Co, Fe and Ni plotted as a function of the homologous temperature T_m/T where T_m is the melting temperature and T is the diffusion annealing temperature. The filled dots, squares and triangles correspond respectively to the $Co_{20}Cr_{20}Fe_{20}Mn_{20}Ni_{20}$, $Co_{10}Cr_{10}Fe_{10}Mn_{10}Ni_{60}$ and $Co_2Cr_2Fe_2Mn_2Ni_{92}$ alloys. The dashed lines are the Arrhenius plots of the $Co_{20}Cr_{20}Fe_{20}Mn_{20}Ni_{20}$ alloy, which were established by Vaidya et al. [14]. The straight lines correspond to the Arrhenius plots of pure Ni, which were published by Monma et al. [20], Vladimirov et al. [21], Bakker et al. [22] and Bronfin et al. [23]. All data for Cr, Co, Fe and Ni are in respective colors, i.e. black, blue, green and orange.

some discrepancies are larger and most likely due to slight differences in processing which induce spurious C or O contamination. However, this comparison illustrates that diffusion coefficients measured in different alloys can reliably be compared, both qualitatively and quantitatively.

Now, the diffusion rates in the HEAs and the dilute solid solutions are compared. The evolution of D_V(Ni) with the alloy composition is different from those of D_V(Cr), D_V(Co) and D_V(Fe). Indeed, D_V(Ni) is approximately constant for the whole range of composition from pure Ni to $Co_{20}Cr_{20}Fe_{20}Mn_{20}Ni_{20}$. On the contrary, D_V(Cr), D_V(Co) and D_V(Fe) decrease when the composition is modified from a dilute solid solution (i.e.: $Co_2Cr_2Fe_2Mn_2Ni_{92}$) to a HEA (i.e.: $Co_{20}Cr_{20}Fe_{20}Mn_{20}Ni_{20}$). This decrease is between 60 and 76% for D_V(Co) and D_V(Fe), respectively, and it appears smooth and continuous. Although more compositions should be studied to get a complete description, a kink in the diffusion behavior between dilute solid solution and HEA is very unlikely to exist.

Furthermore, relatively strong changes of the diffusion rates of solute and solvent atoms are observed between pure Ni and $Co_2Cr_2Fe_2Mn_2Ni_{92}$. For example, the diffusion rates of Cr and Fe are increased by a factor of 3, whereas the diffusion rate of Ni is *decreased* by 20% at 1373 K. It is known that an enhancement of solute diffusion in substitutional FCC diluted alloys corresponds typically to an *increase* of the solvent diffusion rate, too [25,26]; the effect is essentially due to the increase of the vacancy concentration [27]. The opposite trends are clearly seen in Fig. 2b which indicate a sophisticated competition for vacancies by the multi-solute alloying at this temperature.

It is highlighted that the enhancement of the solute diffusion rates in the dilute solution is almost as large as the subsequent deceleration of the diffusion rates between $Co_2Cr_2Fe_2Mn_2Ni_{92}$ and the $Co_{20}Cr_{20}Fe_{20}Mn_{20}Ni_{20}$ HEA. To conclude, at the given absolute temperature of 1373 K, the volume diffusion coefficients of solutes (Cr, Co and Fe) are slower in the high-entropy alloy than in the dilute solid solution. However, the diffusion coefficients are almost the same (within 50%) when HEA and pure Ni are compared; moreover some elements diffuse slower (Ni, Co, Fe) and some are diffusing slightly faster (Cr).

In Fig. 4, the diffusion coefficients are compared using the inverse homologous temperature scale, T_m/T, where T and T_m are the diffusion annealing and melting temperature, respectively. Significant differences between the diffusion rates of the investigated elements in the HEAs and the dilute solid solution are revealed on this scale. Indeed, at the same homologous temperature, the diffusion coefficients in $Co_{10}Cr_{10}Fe_{10}Mn_{10}Ni_{60}$ are by a factor of 3 (Ni) or 8 (Co) larger than the ones in the $Co_{20}Cr_{20}Fe_{20}Mn_{20}Ni_{20}$ HEA ($T_m/T = 1.21$) and the diffusion coefficients of $Co_2Cr_2Fe_2Mn_2Ni_{92}$ are up to 10 (Ni) or 30 (Fe) times larger than those of $Co_{20}Cr_{20}Fe_{20}Mn_{20}Ni_{20}$ ($T_m/T = 1.27$). The difference between the tendencies on the homologous and absolute temperature scales is due to a decrease of the melting temperature between $Co_2Cr_2Fe_2Mn_2Ni_{92}$ and $Co_{20}Cr_{20}Fe_{20}Mn_{20}Ni_{20}$. In future work, the temperature dependencies of the tracer diffusion in $Co_{10}Cr_{10}Fe_{10}Mn_{10}Ni_{60}$ and $Co_2Cr_2Fe_2Mn_2Ni_{92}$ will be determined. The comparison of the calculated activation energy will give more insights on the diffusion mechanism and the element competition for vacancies.

Are these differences significant in order to state the existence of sluggish diffusion in HEAs? The determined retardation of the diffusion rates in HEAs is still within general rules established for substitutional diffusion in FCC metals [28], namely that the diffusion rates of substitutional solutes in FCC matrix are typically within one order of magnitude of that for self-diffusion.[2] Thus, we conclude that the concept of sluggish diffusion cannot be used as a blanket statement for all elements in HEAs and, strictly speaking, the concept is not correct. However, a retardation of the diffusion rate of some

[2] Abnormally slow diffusion of some 3d transition metals in Al [28] is explicitly taken out of consideration in this comparison.

elements in HEAs is most significant if it is referenced to the solid solutions instead of the pure matrix.

In the present work, volume diffusion was measured for the first time in $Co_{10}Cr_{10}Fe_{10}Mn_{10}Ni_{60}$ and $Co_2Cr_2Fe_2Mn_2Ni_{92}$ and re-measured in the well-known equimolar $Co_{20}Cr_{20}Fe_{20}Mn_{20}Ni_{20}$ at 1373 K. The three alloys were shown to form a single-phase FCC solid solution. $Co_2Cr_2Fe_2Mn_2Ni_{92}$ is a conventional dilute solid solution whereas $Co_{20}Cr_{20}Fe_{20}Mn_{20}Ni_{20}$ is a HEA. Thus, the impact of element concentration with no or limited influence of their chemical nature on diffusion in HEAs is addressed.

The main results are the following:

- For the three alloys, the measured tracer diffusion coefficients are in the range of 10^{-15} to 10^{-14} m^2s^{-1} and Cr is the fastest element, followed by Fe, Co and Ni, which is the slowest element at the temperature under investigation.
- At 1373 K, diffusion of Co, Cr and Fe in $Co_{20}Cr_{20}Fe_{20}Mn_{20}Ni_{20}$ is slower than in $Co_2Cr_2Fe_2Mn_2Ni_{92}$ but the differences are comparable with those between pure Ni and $Co_2Cr_2Fe_2Mn_2Ni_{92}$. The changes of the tracer diffusion coefficients are within a factor of three (Co) or even marginal (Ni).
- On a homologous temperature scale, the element diffusion rates in $Co_{20}Cr_{20}Fe_{20}Mn_{20}Ni_{20}$ are by about one order of magnitude slower than in $Co_2Cr_2Fe_2Mn_2Ni_{92}$ at $T_m/T = 1.27$. At this homologous temperature, the diffusion coefficients for $Co_2Cr_2Fe_2Mn_2Ni_{92}$ are within a factor of two of those measured for pure Ni.

We highlight that an increase of the solute concentration while keeping the same elements does not inevitably induce 'sluggish' diffusion at a given temperature. The decrease of the diffusion rates is comparable to differences which are observed between conventional alloys. In contrast, on a homologous temperature scale, tracer diffusion of some elements in HEA can be slower by one order of magnitude compared to that in a conventional dilute solid solutions.

Acknowledgment

Funding by Deutsche Forschungsgemeinschaft (DFG) via SPP2006, project WI 1899/32-1, is gratefully acknowledged.

References

[1] R.E. Hummel, Understanding Materials Science: History, Properties, Applications, Springer Science & Business Media. 2004.
[2] J.-W. Yeh, S.-K. Chen, S.-J. Lin, J.-Y. Gan, T.-S. Chin, T.-T. Shun, C.-H. Tsau, S.-Y. Chang, Adv. Eng. Mater. 6 (2004) 299–303.
[3] B. Cantor, I. Chang, P. Knight, A. Vincent, Mater. Sci. Eng. A 375 (2004) 213–218.
[4] D. Miracle, O. Senkov, Acta Mater. 122 (2017) 448–511.
[5] L. Lilensten, J.-P. Couzinie, L. Perriere, A. Hocini, C. Keller, G. Dirras, I. Guillot, Acta Mater. 142 (2018) 131–141.
[6] B. Gludovatz, A. Hohenwarter, D. Catoor, E.H. Chang, E.P. George, R.O. Ritchie, Science 345 (2014) 1153–1158.
[7] J.-W. Yeh, Ann. Chim. Sci. Mater. 31 (2006) 633–648.
[8] K.-Y. Tsai, M.-H. Tsai, J.-W. Yeh, Acta Mater. 61 (2013) 4887–4897.
[9] S.V. Divinski, A. Pokoev, N. Esakkiraja, A. Paul, Diffusion Foundations 17 (2018) 69–104.
[10] A. Paul, Scr. Mater. 135 (2017) 153–157.
[11] K.-Y. Tsai, M.-H. Tsai, J.-W. Yeh, Scr. Mater. 135 (2017) 158–159.
[12] M. Vaidya, S. Trubel, B. Murty, G. Wilde, S.V. Divinski, J. Alloys Compd. 688 (2016) 994–1001.
[13] M. Vaidya, K. Pradeep, B. Murty, G. Wilde, S. Divinski, Sci. Rep. 7 (2017) 12293.
[14] M. Vaidya, K. Pradeep, B. Murty, G. Wilde, S. Divinski, Acta Mater. 146 (2018) 211–224.
[15] E. Pickering, N.G. Jones, Int. Mater. Rev. 61 (2016) 183–202.
[16] M. Laurent-Brocq, L. Perrière, R. Pirès, Y. Champion, Mater. Des. 103 (2016) 84–89.
[17] G. Bracq, M. Laurent-Brocq, L. Perrière, R. Pirès, J.-M. Joubert, I. Guillot, Acta Mater. 128 (2017) 327–336.
[18] M. Laurent-Brocq, L. Perrière, R. Pirès, F. Prima, P. Vermaut, Y. Champion, Mater. Sci. Eng. A 696 (2017) 228–235.
[19] A. Paul, T. Laurila, V. Vuorinen, S.V. Divinski, Thermodynamics, Diffusion and the Kirkendall Effect in Solids, Springer. 2014.
[20] K. Monma, H. Suto, H. Oikawa, J. Jpn. Inst. Metals 28 (1964) 188–192.
[21] A. Vladimirov, V. Kajgorodov, S. Klotsman, I.S. Trakhtenberg, Fiz. Met. Metalloved. 46 (1978) 1232–1239.
[22] H. Bakker, J. Backus, F. Waals, Phys. Status Solidi B 45 (1971) 633–638.
[23] M. Bronfin, G. Bulatov, I. Drugova, Fiz. Met. Metalloved. 40 (1975) 363–366.
[24] D. Gaertner, J. Kottke, G. Wilde, S.V. Divinski, Y. Chumlyakov, J. Mater. Res. (2018) 1–8. https://doi.org/10.1557/jmr.2018.162.
[25] A. Le Claire, J. Nucl. Mater. 69 (1978) 70–96.
[26] M. Brown, I. Belova, G. Murch, Philos. Mag. 84 (2004) 1105–1112.
[27] J. Philibert, Atom Movements–Diffusion and Mass Transport in Crystals, Les Editions de Physique, 1991.
[28] H. Mehrer, Diffusion in Solids, Springer. 2007.